Stanford Exploration Project, Report 115, May 22, 2004, pages 265–273

Velocity estimation for seismic data exhibiting focusing-effect AVO (Part 4)

Ioan Vlad[1]

ABSTRACT

Focusing-effect AVO (FEAVO) can be eliminated by migrating with a velocity model obtained by Wave-Equation Migration Velocity Analysis (WEMVA). For this specific problem, WEMVA requires the extraction of an image perturbation that contains all and only the FEAVO effects. Such an image perturbation can be generated by using a "discriminate-focus-filter-mask" strategy. A simplified version of the first step of this approach was implemented with acceptable results. A simple, effective and cheap FEAVO detector was also conceived and implemented.

INTRODUCTION

Focusing-effect AVO (FEAVO) is the focusing of seismic wavefield amplitudes through velocity lenses too small to generate fully developed triplications. The amplitude effects are large enough to thwart proper AVO analysis in the affected area (Kjartansson, 1979). The effects can be eliminated by migrating with a velocity model containing the respective lenses (Bevc, 1994). However, the traveltime effects are too small to allow classical velocity analysis approaches such as Dix inversion or traveltime tomography to succeed. New approaches are needed to deal with such small velocity anomalies.

Biondi and Sava (1999) introduced Wave-Equation Migration Velocity Analysis (WEMVA), which finds the unknown part of the true velocity field by optimizing image quality in the angle domain after prestack depth migration. Vlad et al. (2003) have shown on a synthetic dataset that WEMVA resolves the FEAVO-causing velocity anomalies. The solution was verified by showing that the amplitude anomalies disappear after migration with the updated velocity model.

Error can be introduced in WEMVA by two classes of factors. The first one consists of the approximations undertaken by the mathematical and numerical procedures. The second one encompasses the limitations of the ability to transform a given image into an optimal one. In a synthetic dataset, in which the optimal image is known, this second source of error is completely eliminated. This allowed Vlad et al. (2003) to evaluate solely the effect of the first class of error-generating factors (Born approximation, linearized wavefield continuation,

[1]**email:** nick@sep.stanford.edu

etc.), and they found that it is too small to impede WEMVA from resolving the small FEAVO-causing velocity lenses. This paper, on the other hand, deals with eliminating the second class of error-generating factors by obtaining the optimal image in a way that is as error-free as possible.

EXTRACTING THE IMAGE PERTURBATION

WEMVA proceeds in three steps. The first one consists of prestack depth-migrating the data with a starting velocity model, then transforming the image to the angle domain. The second step starts by improving the image so that it is closer to the result of a migration with the correct velocity. The improvement may be performed by straightening the gathers or by smoothing the amplitudes along already flat gathers. The improved image is subtracted from the original one to create an image perturbation. The third step is inverting the image perturbation into a slowness perturbation.

The WEMVA flow presented above is actually the one for the procedure named Target Image Fitting (TIF) WEMVA. In a more radical inversion-theory approach, called Differential Semblance Optimization (DSO) WEMVA, steps 2 and 3 are combined into a single step, with the image improvement being performed by a weight operator during the inversion. In theory, DSO WEMVA will not exhibit the same Born-related problems as TIF WEMVA (Sava and Symes, 2002). However, it assumes that the quality of the image-improvement operator that is embedded as a weight in the inversion can be trusted. I am currently just trying to develop such an image-improvement operator specific to the FEAVO problem, and I need to be able to isolate its effects, so for the time being I will use TIF WEMVA on velocity anomalies inside the Born approximation.

In the context of the FEAVO problem, the image perturbation is the difference between the FEAVO-free image and the original one. I therefore need to eliminate the FEAVO effects from the image. To do so, I have to discriminate between AVO due to focusing and AVO due to actual changes in reflectivity with the incidence angle. I will proceed by first obtaining an estimate of the AVO due to the properties of the reflector.

The variation of amplitudes due to changes in reflectivity with incidence angles lower than 30° has been modeled by Shuey (1985) as follows:

$$R(\theta) = I + G \sin^2(\theta), \tag{1}$$

where I and G are scalars depending only on the physical properties of the materials above and below the reflecting interface. If the amplitudes are picked at a single midpoint-depth location with no FEAVO or illumination problems, and they are plotted as a function of the squared sine of the incidence angle, the values will arrange close to a line with intercept I and gradient G. The presence of FEAVO causes the linear dependence to break, as exemplified in Figure 1. The presence or absence of a linear trend in the ($\sin^2$,amplitude) space is therefore a FEAVO-discriminating criterion, which can be used to eliminate FEAVO. I will have to account also for the superposition of FEAVO and reflector-caused AVO. At each midpoint-depth location, I

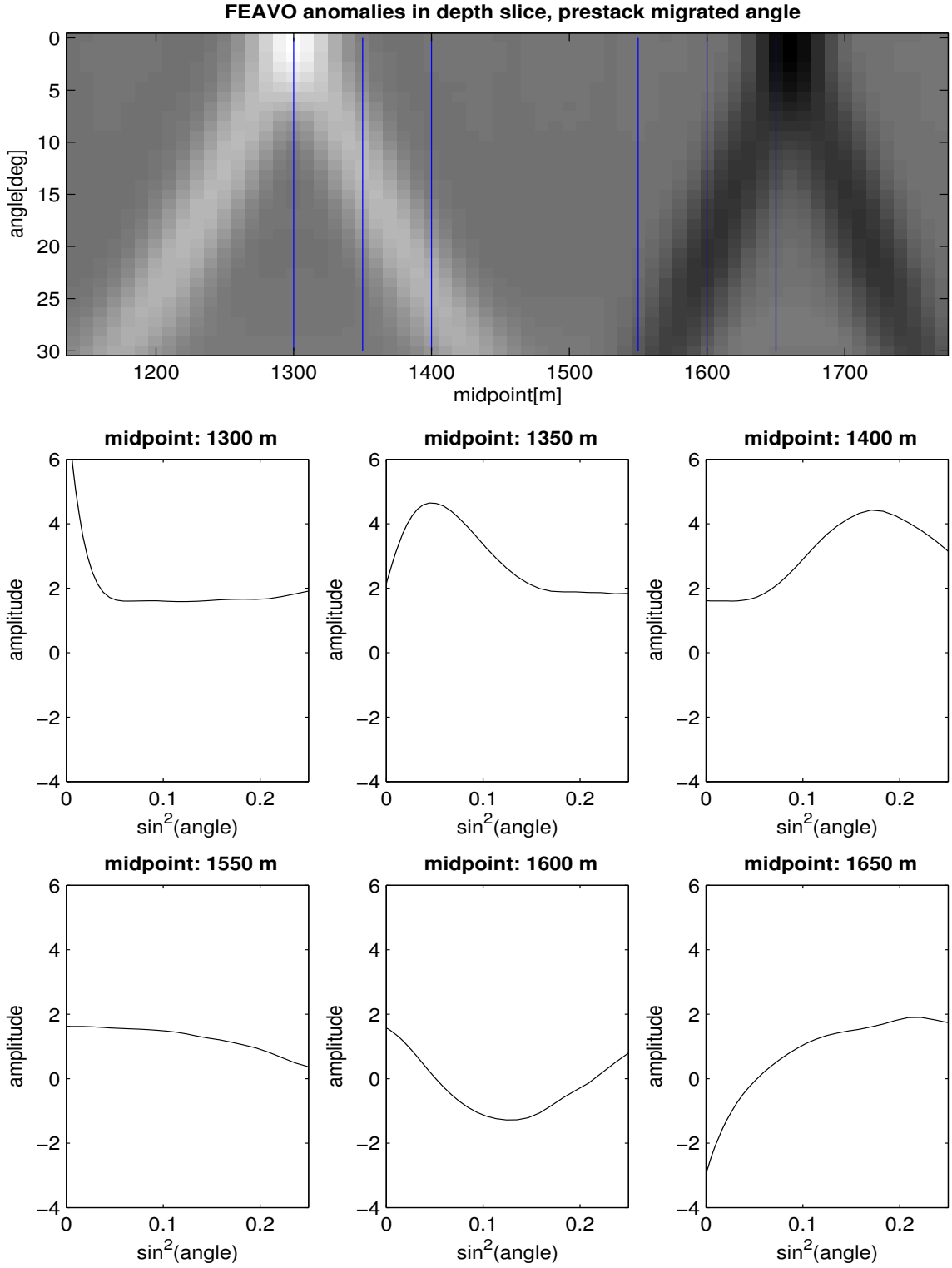

Figure 1: **Top panel:** Midpoint-angle depth slice from the prestack migrated synthetic dataset shown in Figure 1 of Vlad et al. (2003). **Bottom panels:** Amplitudes at midpoints marked by vertical thin lines in the upper panel. nick1-examine_FEAVO [CR]

will compute the most plausible reflector-caused AVO as a linear trend in the ($\sin^2$,amplitude) space, and I will obtain FEAVO by subtracting this trend from the image.

The challenge is now fitting to the data at each midpoint-depth location a linear trend in the ($\sin^2$,amplitude) space. The trend should be as close as possible to that of the reflector-caused AVO, even when focusing effects are present. I will consider only the angles up to 30°. After that, the accuracy of the angle-gather amplitudes decreases, unless the offsets are extremely densely sampled, which would increase the costs of the migrations in WEMVA too much. Also, after 30°, the two-term Shuey approximation of reflector-caused AVO stops working. I have experimented with his three-term formula for larger angles. The extra degree of freedom allowed for a curve that fitted everything, including the FEAVO effects at angles lower than 30°. I have therefore to decided to use only the two-term formula on angles under 30°.

The best way to fit the linear trend would be to formulate the fit as a 2-D inverse problem, penalizing nonphysical variations of AVO along the midpoint or along the reflector. While I intend to do so in the future, I experimented for the time being with a 1-D approach mapped in Figure 2. At each (midpoint, depth) location I fitted by least-squares a straight line through

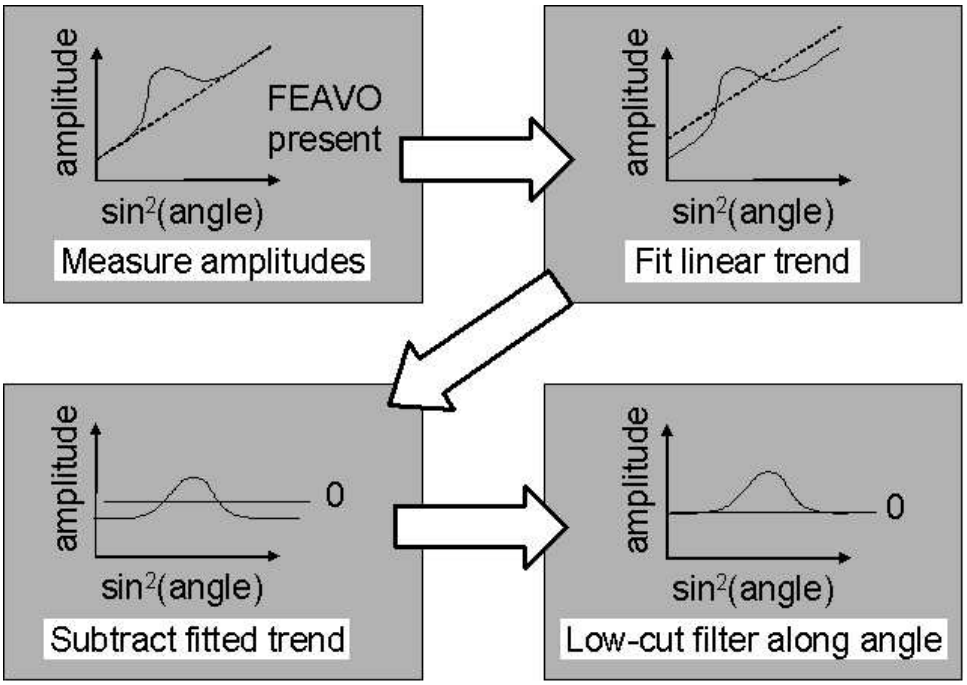

Figure 2: 1-D FEAVO extraction flowchart. nick1-extract1D_flow [NR]

the [reflectivity, $\sin^2$(angle)] pairs. I then subtracted the linear trend and applied a low-cut filter along angle. A depth slice from the results of the FEAVO extraction, together with the corresponding true FEAVO anomalies, is shown in Figure 3. The extracted anomalies are closer in morphology to the true FEAVO in the optimal image perturbation. Also, the extraction worked up to 30°, in contrast with the previous image-processing-based technique proposed by Vlad et al. (2003), which only worked up to 21°.

A 2-D extraction procedure in which the intercept and gradient would vary more smoothly

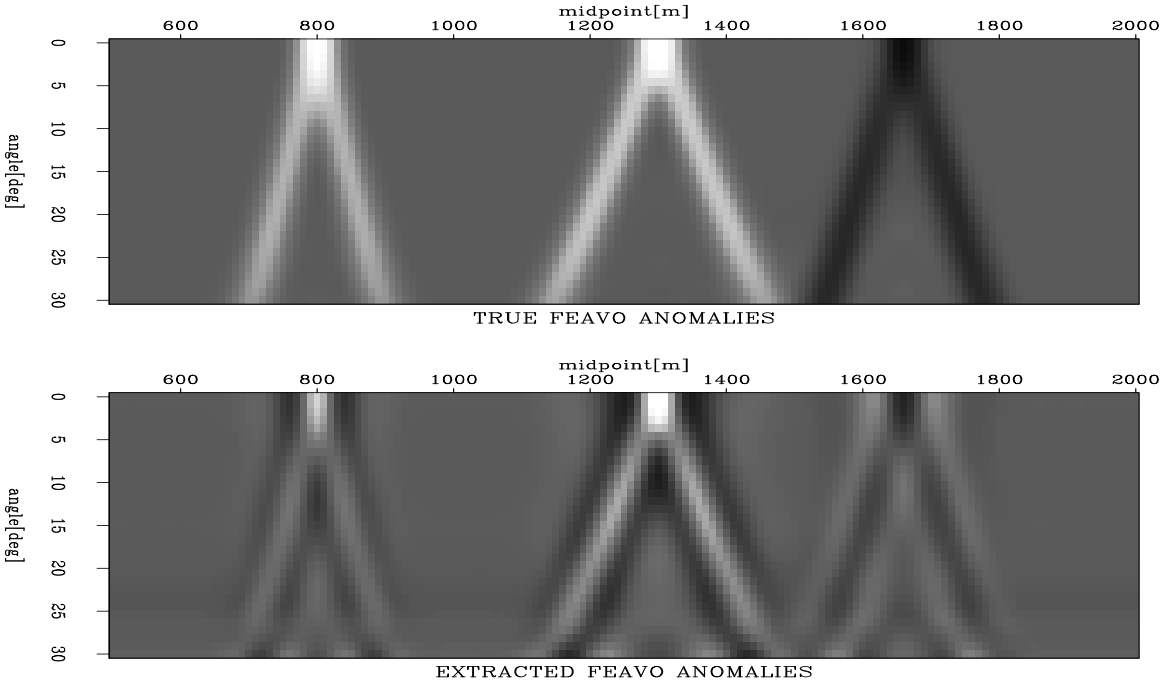

Figure 3: **Top panel:** Depth slice from the optimal angle-domain image perturbation in the top panel of Figure 6 of Vlad et al. (2003)). **Bottom panel:** FEAVO anomalies extracted by applying the workflow in Figure 2 to the image built by migrating with a constant velocity the dataset in Figure 1 of Vlad et al. (2003). nick1-extractFEAVO [CR]

along the midpoint would make it possible to eliminate in the future the low-pass filter step, which is responsible for the reverse-polarity "borders" around the extracted anomalies. However, the results of the 1-D extracting procedure may still provide some valuable insight into the effectiveness of FEAVO extracting procedure, given that the "unfair" advantage of the lack of noise is compensated by the simplicity of the 1-D extraction.

The slowness update produced by inverting the extracted image perturbation is displayed in Figure 4. The slowness update produced this way puts anomalies with the correct polarities in the correct places. The shape of the anomalies could nevertheless be improved with the use of a 2-D FEAVO extraction procedure.

The method presented in this paper discriminates FEAVO on the basis of a local property—nonlinear variation with the squared sine of the angle. FEAVO anomalies, however, are correlated in tent-like shapes throughout the prestack volume, as shown in Figures 3, 4 and 9 in Vlad (2002). That paper proposed a "focus-filter-spread" approach to discriminate FEAVO from uncorrelated amplitude effects. The shapes of the anomaly surfaces in the prestack volume can be precomputed as functions of the known velocity. Summation along them would highlight the anomalies; only the "bright stars" would be kept. Then, the de-noised Radon-space image would be spread along the surfaces, to keep only the FEAVO anomalies in the image perturbation. Vlad et al. (2003) identified a major difficulty with this approach: the alternating polarities in the wavelet would lead to summed values canceling each other. The

Figure 4: Slowness backprojection of the image perturbation using one nonlinear WEMVA iteration, with an unregularized solver. nick1-slow_proj [CR]

obvious solution—taking the unsigned values—would, however, lead to the inability to discriminate between positive and negative velocity anomalies, and to the inversion process never converging if the data contains FEAVO-generating velocity anomalies of more than one sign.

The conundrum of FEAVO extraction based on its global properties can however be broken by using a procedure that I present below. Instead of a "focus-filter-spread" approach, I will use a "discriminate-focus-filter-mask" one. I will first process the prestack volume through a FEAVO discriminator based on the local properties of the anomalies. Then, as in the "focus-filter-spread" approach, I will square or take the modulus of the values in the prestack volume, sum along precomputed velocity-dependent surfaces, filter to keep only the "bright stars" in the Radon domain, then spread back. But instead of feeding the result of spreading into the inversion, I will use it as a mask that I will apply to the result of local property-based FEAVO discrimination. That will filter out all areas with amplitude variations that are nonlinear, but are not FEAVO (because they do not correlate vertically and laterally in the known tent-shape). Since the synthetic dataset used in this paper does not have non-FEAVO amplitude departures from the Shuey (1985) model, it represents a good benchmark for the accuracy of the inversion, even in the absence of the de-noising "focus-filter-mask" step.

AUTOMATIC FEAVO DETECTION

The automatic FEAVO-discriminating procedure outlined in the previous section offers a ready solution to an older problem: FEAVO detection. Until now, the only way to find whether the amplitudes at the reflector were corrupted by focusing effects was the method used by Kjartansson (1979). First, the interpreter would have to become suspicious that the AVO in his region of interest exhibited variations too strong and abrupt to be due to the rock properties expected at that interface. The dataset would be sent back to processing, which would sum the absolute values of the samples in the 2-D prestack line along time, and examine the midpoint-offset image looking for the specific "V" shapes of the anomalies. Since it is not to be expected that such a labor-intensive, custom procedure was undertaken routinely, compromised AVO measurements were the likely result.

FEAVO, however, can be detected and flagged automatically during processing in a much simpler way. Figure 2 depicts the removal of a linear trend from FEAVO-affected data. If the same workflow is applied to data that is not affected by FEAVO, the residual after subtraction of the trend will be very close to zero everywhere. High values in the variance of the residuals will therefore flag the presence of FEAVO. Figure 5 shows the result of automatic FEAVO detection, which is no longer a 5-D cube, but a 3-D one, reducing the volume of data to be examined by orders of magnitude through elimination of the offset axes. The presence of FEAVO anomalies is highly visible. I need not even do a good job of finding the values of the intercept and gradient. All that matters for detection is that the amplitude values in focusing-affected areas do not vary linearly with the squared sine of offset, and therefore no straight line whatsoever will approximate them well. The procedure is also quite cheap computationally.

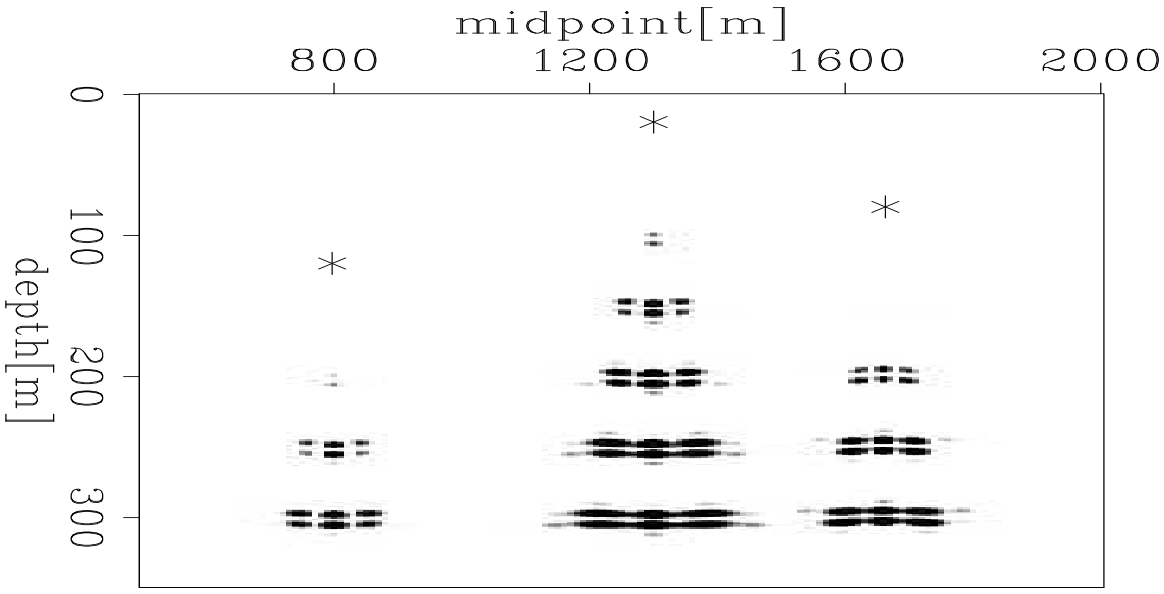

Figure 5: FEAVO anomalies flagged in the midpoint-depth space by the automatic detection procedure. The stars denote the location of the lenses causing the focusing. nick1-anoloc [CR]

I could build an "anomaly locator" by summing Radon-transform-style the output of the FEAVO detector inside the bounds of precomputed, velocity-dependent, FEAVO-effect paths. That, however, would not give the magnitude of the velocity anomalies, so it would be of little use in eliminating the amplitude effects in the prestack volume.

CONCLUSIONS

I have identified a "discriminate-focus-filter-mask" strategy for constructing an image perturbation for WEMVA's application to the FEAVO problem. I implemented, with acceptable results, a simplification of the first step of this approach—FEAVO discrimination based on local characteristics. I built and implemented an effective process for performing FEAVO detection in a much simpler and cheaper manner than the current practice.

ACKNOWLEDGMENTS

I thank Paul Sava for meaningful discussions and for software assistance.

REFERENCES

Bevc, D., 1994, Near-surface velocity estimation and layer replacement: SEP–**80**, 361–372.

Biondi, B., and Sava, P., 1999, Wave-equation migration velocity analysis: SEP–**100**, 11–34.

Kjartansson, E., 1979, Analysis of variations in amplitudes and traveltimes with offset and midpoint: SEP–**20**, 1–24.

Sava, P., and Symes, W. W., 2002, A generalization of wave-equation migration velocity analysis: SEP–**112**, 27–36.

Shuey, R. T., 1985, A simplification of the Zoeppritz equations: Geophysics, **50**, no. 4, 609–614.

Vlad, I., Biondi, B., and Sava, P., 2003, Velocity estimation for seismic data exhibiting focusing-effect AVO (Part 3): SEP–**114**, 101–109.

Vlad, I., 2002, Velocity estimation for seismic data exhibiting focusing-effect AVO (Part 2): SEP–**112**, 47–64.